arXiv:1401.0738v2 [cond-mat.mes-hall] 14 Mar 2015

Andreev states in the spin-symmetric solution of a quantum dot attached to superconducting leads

V. Janiš*
Institute of Physics, Academy of Sciences of the Czech Republic, Na Slovance 2, CZ-18221 Praha 8, Czech Republic and Fulbright Scholar at Department of Physics and Astronomy, Louisiana State University, Baton Rouge, LA 70803, USA

V. Pokorný
Institute of Physics, Academy of Sciences of the Czech Republic, Na Slovance 2, CZ-18221 Praha 8, Czech Republic and Theoretical Physics III, Center for Electronic Correlations and Magnetism, Institute of Physics, University of Augsburg, D-86135 Augsburg, Germany

M. Žonda
Department of Condensed Matter Physics, Faculty of Mathematics and Physics, Charles University in Prague, Ke Karlovu 5, CZ-12116 Praha 2, Czech Republic

(Dated: March 17, 2015)

A quantum dot with Coulomb repulsion attached to left and right superconducting leads is studied via the perturbation expansion in the interaction strength. We use the Nambu formalism and the standard many-body diagrammatic representation of the impurity Green functions. We formulate the perturbation expansion in the spectral representation so that to be able to separate contributions of the isolated Andreev bound states and from those of the continuous band states. We resolve exactly the spin-symmetric state in the asymptotic limit with Andreev states approaching the Fermi energy. We demonstrate that the spin-symmetric state reaches saturation at zero temperature at a critical interaction at which the Andreev states merge and freeze at the Fermi energy. There is no solution above this critical interaction with Andreev states split from the Fermi energy unless external magnetic field breaking the spin reflection symmetry is applied and degeneracy of the ground state lifted.

PACS numbers: 72.15.Qm, 74.50.+r, 73.63.Kv

I. INTRODUCTION

Nanostructures attached to leads with specific properties display interesting and important quantum effects at low temperatures. Much attention, both from experimentalists[1] and theorists,[2] has been paid in recent years to a quantum dot with well separated energy levels attached to BCS superconductors. In particular, behavior of the supercurrent (Josephson current) that can flow through the impurity without any external voltage bias between the two superconducting leads in equilibrium was in the center of interest.[3–5] The Josephson current is in the non-interacting or weakly interacting dot proportional to the sine of the phase difference between the left and right superconductor. But when it goes through the impurity with a tangible Coulomb repulsion it undergoes a transition signaled by the reversal of the sign of the current.[6–10] Full and unambiguous theoretical picture of this quantum phase transition has not yet been reached. There is general consensus that the sign reversal of the Josephson current has origin in a transition from a spin-singlet state (0-phase), where the supercurrent is positive, to a spin-doublet state (π-phase) where the supercurrent is smaller in value and negative.[11,12] Weak-coupling mean-field static solutions obtain a $0-\pi$ transition in the Josephson current as a consequence of a first-order transition from a spin-symmetric to a spin-polarized state.[12–14] This Hartree-Fock solution does not contain dynamical fluctuations and its conclusion about the existence of a magnetic order in the π-phase is not fully reliable. More advanced, mostly numerical approaches such as numerical renormalization group (NRG),[15–17] Monte-Carlo simulations,[18,19] (semi)analytical methods based on expansion around the atomic limit[20–22], or formalisms specialized on the strongly correlated systems such as slave-particles[23,24] and functional renormalization group (fRG)[25] produce a continuous $0-\pi$ transition.

The question whether the $0-\pi$ transition is a consequence of a transition from a spin-symmetric to a spin-polarized state is subtle and essentially demands knowledge of spectral properties of the one-electron propagator on the impurity. Numerical methods and most of the analytic approaches are formulated in the Matsubara formalism within which spectral properties are not directly accessible. A few approaches have tried to address the impurity Green function for real frequencies and to understand the $0-\pi$ transition from changes of spectral properties.[14,19,22,26–28] The principal result of these analyses is that the $0-\pi$ transition is a consequence of a crossing of the gap states. Due to the proximity effect the gap

of the superconducting leads is imposed on the impurity spectrum, while the original atomic levels for the electron and the hole of the dot transform to Andreev bound states (ABS). There are two Andreev (bound and anti-bound) states in the singlet spin-symmetric phase while other two emerge in the spin-polarized phase. The Andreev states are always symmetrically distributed around the Fermi energy (center of the gap). At the transition point the existing two ABS from the 0-phase reach the Fermi energy and are expected to interchange their positions in the π-phase. These conclusions were confirmed experimentally via scanning tunneling spectroscopy.[17,29] A recent analysis of a quantum dot in the weak-coupling regime demonstrated that already second order of perturbation theory in the spin-symmetric state gives unprecedented accuracy in determining the $0-\pi$ transition comparable with the Numerical Renormalization Group (NRG) when the zero-temperature transition is determined from the point where the energies of the Andreev states merge at the Fermi energy.[30] This approach, however, does not allow to continue the solution beyond this critical point to the π-phase and unfortunately cannot decide about the crossing of the Andreev states in the spin-symmetric (non-magnetic) solution.

The behavior of the Andreev states is important for the determination of the supercurrent through the impurity. The Josephson current is generally dependent on the phase difference between the attached superconducting leads. The Andreev states have the dominant contribution to the supercurrent in the 0-phase. When the bound and anti-bound Andreev states reach the Fermi energy the contributions from the bound electrons and bound holes to the Josephson current mutually compensate each other and upon crossing the flow of the supercurrent flips to the opposite direction, the hole dominated regime.

The existing spectral analysis has not yet resolved the question whether the π-phase can be described within a spin-symmetric theory. The weak-coupling Hartree-Fock approximation and expansion beyond it lead to a spin-polarized π-phase, while the numerical solutions connect the π-phase with a degenerate state but still without equilibrium (static) spin polarization. The question whether we can obtain the $0-\pi$ transition where the Andreev bound states cross without breaking spin-reflexion symmetry remains to be answered.

It is the aim of this paper to analyze the perturbation theory in the spin-symmetric state with a non degenerate ground state. We use the standard diagrammatic representation of the expansion in the Coulomb repulsion in the Nambu formalism and Matsubara frequencies. All the terms of the expansion are eventually analytically continued to real frequencies obtaining thereby their spectral representation. We explicitly single out contributions from the gap states to the self-energy in the gap of the impurity one-electron Green function where both are real. We derive the asymptotic behavior of the full solution with energies of the Andreev states approaching the Fermi level. We show that above a critical interaction the Andreev states cannot peel off from the Fermi level and the spin-symmetric solution with a non-degenerate ground state does not allow for crossing of Andreev states. Apart from that we prove that a solution with merged bound and anti-bound Andreev states can coexist with the solution with the split Andreev states.

II. MODEL HAMILTONIAN AND THE NAMBU FORMALISM

A single impurity is used to simulate the nanowire with separated energy levels connecting superconducting leads in the experimental setup.[15,17,18,31] The Hamiltonian of the system consisting of a single impurity attached to left-right BCS superconductors is

$$\mathcal{H} = \mathcal{H}_{dot} + \sum_{s=R,L} (\mathcal{H}^s_{lead} + \mathcal{H}^s_c) \ , \tag{1}$$

where the impurity Hamiltonian is a single-level atom with the level energy $\pm\epsilon$ for single electron (hole) and Coulomb repulsion U

$$\mathcal{H}_{dot} = \epsilon \sum_\sigma d^\dagger_\sigma d_\sigma + U d^\dagger_\uparrow d_\uparrow d^\dagger_\downarrow d_\downarrow \ . \tag{2}$$

The Hamiltonian of the leads is

$$\mathcal{H}^s_{lead} = \sum_{\mathbf{k}\sigma} \varepsilon(\mathbf{k}) c^\dagger_{s\mathbf{k}\sigma} c_{s\mathbf{k}\sigma} - \Delta_s \sum_{\mathbf{k}} (e^{i\Phi_s} c^\dagger_{s\mathbf{k}\uparrow} c^\dagger_{s-\mathbf{k}\downarrow} + \text{H.c.}) \tag{3}$$

with $s = L, R$ denoting left, right lead. Finally, the hybridization term for the contacts reads

$$\mathcal{H}^s_c = -t_s \sum_{\mathbf{k}\sigma} (c^\dagger_{s\mathbf{k}\sigma} d_\sigma + \text{H.c.}) \ . \tag{4}$$

We introduce Nambu spinor representation to describe Cooper pairs and anomalous functions breaking charge conservation. We denote spinors on the impurity site

$$\widehat{\phi}_\sigma = \begin{pmatrix} d_\sigma \\ d^\dagger_{-\sigma} \end{pmatrix} \quad , \quad \widehat{\phi}^\dagger_\sigma = \begin{pmatrix} d^\dagger_\sigma & d_{-\sigma} \end{pmatrix} \ . \tag{5}$$

The individual degrees of freedom of the leads are unimportant for the studied problem and are generally integrated out. We are left with only the active variables and functions on the impurity. The fundamental function is the one-electron impurity Green function measuring (imaginary) time fluctuations that in the Nambu formalism is a 2×2 matrix

$$\begin{aligned} &\widehat{G}_\sigma(\tau - \tau') \\ &= -\begin{pmatrix} \langle \mathbb{T}\left[d_\sigma(\tau) d^\dagger_\sigma(\tau')\right]\rangle \ , & \langle \mathbb{T}\left[d_\sigma(\tau) d_{-\sigma}(\tau')\right]\rangle \\ \langle \mathbb{T}\left[d^\dagger_{-\sigma}(\tau) d^\dagger_\sigma(\tau')\right]\rangle \ , & \langle \mathbb{T}\left[d^\dagger_{-\sigma}(\tau) d_{-\sigma}(\tau')\right]\rangle \end{pmatrix} \\ &= \begin{pmatrix} G_\sigma(\tau - \tau') \ , & \mathcal{G}_{-\sigma}(\tau - \tau') \\ \mathcal{G}^*_\sigma(\tau - \tau') \ , & G^*_{-\sigma}(\tau - \tau') \end{pmatrix} \end{aligned} \tag{6}$$

correlating appearance of electrons and holes with specific spin on the impurity. We introduced particle $G_\sigma, \mathcal{G}_\sigma$ and hole $G^*_\sigma, \mathcal{G}^*_\sigma$ Green functions for individual spins. They are connected by symmetry relations $G^*_\sigma(\tau) = -G_\sigma(-\tau) = -G_\sigma(\tau)^\dagger$, $\mathcal{G}_\sigma(\tau) = -\mathcal{G}_{-\sigma}(-\tau)$, $\mathcal{G}^*_\sigma(\tau) = -\mathcal{G}^*_{-\sigma}(-\tau)$, and $\mathcal{G}^*_\sigma(\tau) = \mathcal{G}_\sigma(-\tau)^\dagger$ since the normal Green function is odd while the anomalous is an even function of the imaginary time.

The problem can be exactly solved for an impurity without onsite interaction, $U = 0$. Due to energy conservation it is convenient to use the Fourier transform from (imaginary) time to frequency (energy) where the Green function can analytically be continued to complex values. The matrix of the inverse Green function for a complex energy z with identical left and fright superconductors reads

$$\widehat{G}_0^{-1}(z) = \begin{pmatrix} z[1+s(z)] - \epsilon \ , & \Delta\cos(\Phi/2)s(z) \\ \Delta\cos(\Phi/2)s(z) \ , & z[1+s(z)] + \epsilon \end{pmatrix}, \quad (7)$$

where

$$s(z) = \frac{i\Gamma_0}{\zeta}\mathrm{sgn}(\Im z). \quad (8)$$

is the "hybridization self-energy", that is, a dynamical renormalization of the impurity energy level due to the hybridization to the superconducting leads. We approximated the Green function in the leads by its value at the Fermi energy and introduced an effective hybridization strength $\Gamma_0 = 2\pi t^2\rho_0$. We denoted $\Phi = \Phi_L - \Phi_R$ the difference between the phases of the left and right superconducting leads and ρ_0 the density of states of the lead electrons at the Fermi energy. To represent explicitly the hybridization self-energy we introduced a new complex number $\zeta = \xi + i\eta$ derived from the complex energy $z = x + iy$ by a quadratic equation $\zeta^2 = z^2 - \Delta^2$. Thereby the following convention for the complex square root has been used

$$\xi\eta = xy, \quad \mathrm{sgn}(\xi) = \mathrm{sgn}(x), \quad \mathrm{sgn}(\eta) = \mathrm{sign}(y) \ . \quad (9)$$

III. PERTURBATION EXPANSION IN THE INTERACTION STRENGTH

A. One-particle functions

The full inclusion of the Coulomb repulsion on the impurity cannot be exactly (analytically) performed and we hence must resort to approximations. A systematic way to assess the impact of the Coulomb repulsion on equilibrium properties is a renormalized perturbation expansion. The best way to control the individual contributions from the perturbation expansion is to represent them diagrammatically.

We start with the Nambu spinor of the impurity propagator that we represent by solid lines decorated by arrows

$$\begin{pmatrix} G_\sigma(\tau-\tau') \ , & \mathcal{G}_{-\sigma}(\tau-\tau') \\ \mathcal{G}^*_\sigma(\tau-\tau') \ , & G^*_{-\sigma}(\tau-\tau') \end{pmatrix}$$

(10)

We keep time (charge) propagation (from left to right) in the diagrammatic representation and assign spin to the propagators. Whereby the upper/lower line corresponds to spin up/down. We can construct standard Feynman many-body diagrams for processes induced by the Coulomb interaction of the electrons on the impurity between two superconducting leads. The Coulomb interaction will be represented via a wavy line. Since the interaction is static, the interaction wavy line is always vertical. Before we start to analyze the diagrammatic contributions from the perturbation expansion we resume basic exact relations.

The impact of the Coulomb repulsion on the Green function is included in a matrix self-energy $\hat{\Sigma}(z)$ so that the full inverse propagator in the spin-symmetric situation reads $\widehat{G}^{-1}(z) = \widehat{G}_0^{-1}(z) - \widehat{\Sigma}(z)$. Its explicit component representation is

$$\widehat{G}^{-1}(z) = \begin{pmatrix} z[1+s(z)] - \epsilon - \Sigma(z) \ , & \Delta_\Phi\left[s(z) - \mathcal{S}(z)\right] \\ \Delta_\Phi\left[s(z) - \mathcal{S}^*(z)\right] \ , & z[1+s(z)] + \epsilon - \Sigma^*(z) \end{pmatrix}. \quad (11)$$

We denoted Σ and $\mathcal{S}$ the normal and anomalous parts of the interaction-induced electron self-energy, while Σ^* and $\mathcal{S}^*$ are the self-energies of the hole. The electron-hole symmetry relations for the unperturbed Green function read in the (complex) energy representation

$$G^*(z) = -G(-z) \quad \text{and} \quad \mathcal{G}^*(z) = \mathcal{G}(-z) \ . \quad (12)$$

Consequently, the same relations hold for the self-energies

$$\Sigma^*(z) = -\Sigma(-z) \quad \text{and} \quad \mathcal{S}^*(z) = \mathcal{S}(-z) \ . \quad (13)$$

If we denote $D(z) = \det[\hat{G}^{-1}(z)]$, the determinant of the inverse Green function, then with the the electron-hole symmetry we obtain

$$D(z) = z^2\left[1+s(z)\right]^2 - \left[\epsilon + \Sigma(z)\right]\left[\epsilon + \Sigma(-z)\right] - \Delta_\Phi^2\left[s(z) - \mathcal{S}(z)\right]\left[s(z) - \mathcal{S}(-z)\right] \quad (14)$$

and the full one-particle Green function can be represented with the above notation as

$$\widehat{G}(z) = \frac{1}{D(z)} \times \begin{pmatrix} z[1+s(z)] + \epsilon + \Sigma(-z) \ , & -\Delta_\Phi\left[s(z) - \mathcal{S}(z)\right] \\ -\Delta_\Phi\left[s(z) - \mathcal{S}(-z)\right] \ , & z[1+s(z)] - \epsilon - \Sigma(z) \end{pmatrix}. \quad (15)$$

The unperturbed ($U = 0$) impurity Green function is

$$\widehat{G}^{(0)}(z) = \frac{1}{D_0(z)} \begin{pmatrix} z[1+s(z)] + \epsilon \ , & -\Delta_\Phi s(z) \\ -\Delta_\Phi s(z) \ , & z[1+s(z)] - \epsilon \end{pmatrix}. \tag{16}$$

where we denoted $\Delta_\Phi = \Delta \cos(\Phi/2)$ and introduced

$$D_0(z) = z^2(1+s(z))^2 - \epsilon^2 - \Delta_\Phi^2 s(z)^2$$

the determinant of the matrix of the inverse unperturbed impurity Green function.

B. Two-particle vertex functions

We introduce a similar notation for the two-particle vertex and arrange the two-particle diagrams in the perturbation expansion. We use the electron-hole notation, which means that the fundamental (normal) vertex contains one electron and one hole. We must assign three independent dynamical variables, Matsubara frequencies in this case, to four end points. We do it for the normal vertex in the following way

$X(i\omega_n, i\omega_{n'}; i\nu_m) =$

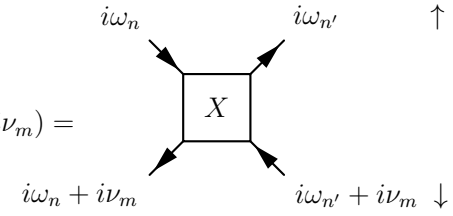

. (17)

The anomalous vertex has a different assignment of frequencies, since the corners of the vertex are connected via diagonals, anomalous Green functions.

$\mathcal{X}(i\omega_n, i\omega_{n'}; i\nu_m) =$

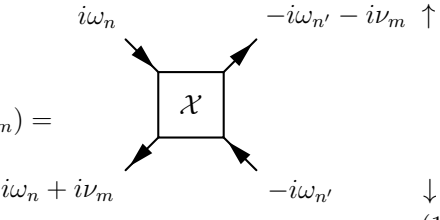

. (18)

The convention of attaching the dynamical variables is as follows. The particles propagate from left to right, the holes from right to left. The arrow indicates propagation of the charge and the transfer energy $-\nu_m$ is the total incoming energy of the particle pair. All possible singlet vertex functions in the superconducting ground state (electron-hole, electron-electron and hole-hole) are plotted in Fig. 1. They differ in orientations of upper and/or lower lines. The anomalous vertices need not conserve charge.

The one-electron propagators in the ordered state with anomalous functions are 2×2 matrices. Two-particle propagators in full generality are then 4×4 matrices.[32] With matrix vertices we describe all possible scatterings of two simultaneously propagating particles. We generally have three different scattering channels, nonequivalent representations of the full two-particle vertex via Bethe-Salpeter equations.[33] Each Bethe-Salpeter equation determines a two-particle irreducibility. We denote L and $\mathcal{L}$ normal and anomalous two-particle irreducible vertices, respectively and K and $\mathcal{K}$ the corresponding full ones. If we resort to only spin-singlet propagation of two particles, that is, we neglect connections of the vertices by the lines of the same spin or by lines not conserving spin, we manage to describe the two-particle scatterings with only 2×2 matrices. In this case we have two fundamental types of Bethe-Salpeter equations determining the electron-hole and electron-electron irreducibility.[34]

The general Bethe-Salpeter equation in the electron-hole scattering channel can be diagrammatically represented as a matrix equation

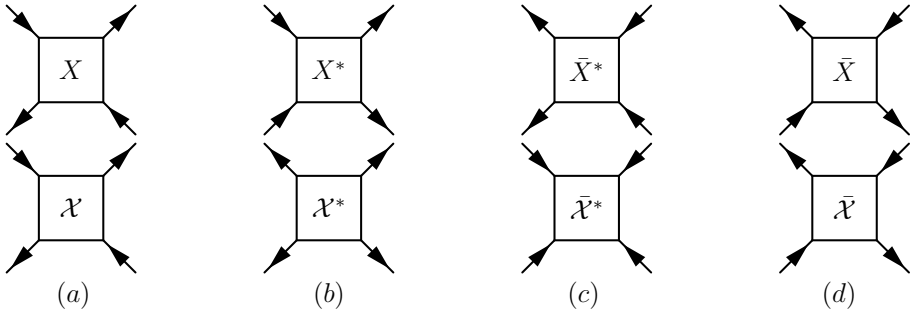

FIG. 1: Normal (X) and anomalous ($\mathcal{X}$) singlet vertices. The upper line carries spin up and the lower one spin down. We took the electron-hole representation as the fundamental one. Notice that anomalous vertices (a) and (c) conserve charge while vertices (b) and (d) not. The conserving normal and anomalous vertices differ only in the way the outer corners are interconnected inside the vertex, via either normal or anomalous propagators.

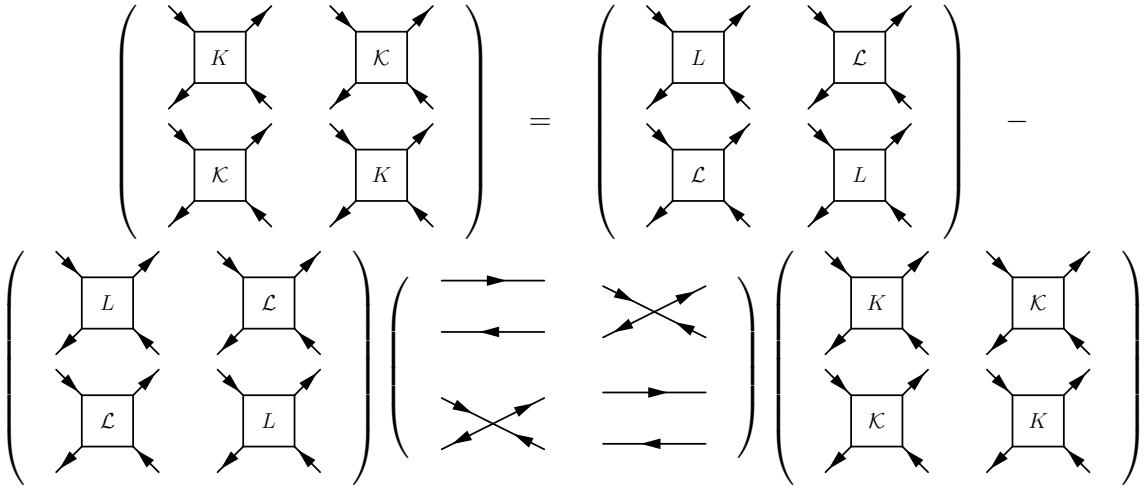

(19)

where again the upper line carries spin up and the lower one spin down. Vertices L and $\mathcal{L}$ are irreducible in the electron-hole channel, it means that they are sums of connected diagrams that cannot be split into two disconnected parts by cutting a singlet electron-hole propagation (antiparallel lines), represented by the middle matrix on the second line in Eq. (19). It is interesting to note that the Berthe-Salpeter equation in the singlet electron-hole channel does not contain the anomalous vertex not conserving charge.

Knowing the two-particle vertices K and $\mathcal{K}$ we construct the corresponding one-particle self-energy via a Schwinger-Dyson equation. It reads for the normal part of the self-energy

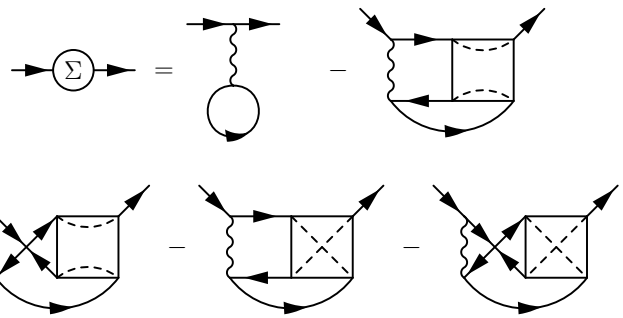

(20)

while the diagrammatic representation for the anomalous

self-energy is

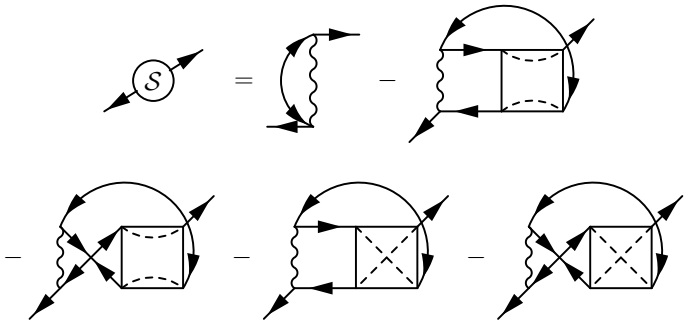

(21)

We used dashed lines within the full vertex functions to distinguish normal vertex K (horizontal lines) from the anomalous one $\mathcal{K}$ (diagonal lines). These internal lines indicate the way the corners of the vertices are interconnected by fermionic propagators.

IV. SPECTRAL REPRESENTATION AND ANDREEV BOUND STATES

A. Analytic continuation to real frequencies of Matsubara sums

General diagrammatic representation with its rules directly gives expressions in Matsubara frequencies. The Matsubara representation on the temperature axis carries no direct information about the gap and the Andreev states. To control the Andreev states and their dependence on the interaction strength we must analytically continue the sums over Matsubara frequencies to spectral integrals over real frequencies. The sums over fermionic and bosonic Matsubara frequencies to be analytically continued generally are

$$X(i\nu_m) = \frac{1}{\beta}\sum_n A(i\omega_n + i\nu_m)B(i\omega_n)\ , \qquad (22)$$

$$C(i\omega_n) = \frac{1}{\beta}\sum_m Z(i\nu_m)B(i\omega_n + i\nu_m)\ . \qquad (23)$$

Their spectral representations, assuming vanishing of the functions at infinity, are

$$X(z) = -\int_{-\infty}^{\infty}\frac{d\omega}{\pi}f(\omega)\left[\Im A(\omega^+)B(\omega+z) + \Im B(\omega^+)A(\omega-z)\right] \qquad (24)$$

and

$$\omega C(z) = \mathcal{P}\int_{-\infty}^{\infty}\frac{d\omega}{\pi}\left[b(\omega)\Im Z(\omega^+)B(\omega+z) - f(\omega)\Im B(\omega^+)Z(\omega-z)\right] \qquad (25)$$

where $f(\omega)$ and $b(\omega)$ are Fermi-Dirac and Bose-Einstein distributions. We abbreviated $\omega^+ = \omega + i0^+$.

The unperturbed one-electron Green functions have a gap around the Fermi energy $[-\Delta, \Delta]$ and two poles at $\pm\omega_0$, $0 \le \omega_0 < \Delta$. Since the hybridization self-energy $s(z)$ has a square-root singularity at the gap/band edges, the gap is fixed and does not depend on the interaction strength. The poles and band edges of the higher-order Green functions do depend on the interaction strength. We hence must be careful when treating the two-particle functions in the spectral representation.

The sum over the fermionic Matsubara frequencies for the one-particle function can then be rewritten in the spectral representation

$$\frac{1}{\beta}\sum_n F(i\omega_n) \to -\left[\int_{-\infty}^{-\Delta} + \int_{\Delta}^{\infty}\right]\frac{d\omega}{\pi}f(\omega)\Im F(\omega+i0) + \sum_i f(\omega_i)\,\mathrm{Res}[F,\omega_i] \qquad (26)$$

containing an integral over the band states and a sum over isolated poles within the gap. Using formula (24) we can represent the two-particle bubbles. We resort in further reasoning to zero temperature. The bubble with normal propagators reads

$$\chi(z) = -\int_{-\infty}^{-\Delta}\frac{d\omega}{\pi}\left[\Im G(\omega^+)G(\omega-z) + \Im G(\omega^+)G(\omega+z)\right] + \mathrm{Res}[G,-\omega_0]G(-\omega_0-z) + \mathrm{Res}[G,-\omega_0]G(-\omega_0+z) \qquad (27)$$

and the anomalous one is

$$\psi(z) = -\int_{-\infty}^{-\Delta}\frac{d\omega}{\pi}\left[\Im \mathcal{G}(\omega^+)\mathcal{G}(\omega-z) + \Im \mathcal{G}(\omega^+)\mathcal{G}(\omega+z)\right] + \mathrm{Res}[\mathcal{G},-\omega_0]\mathcal{G}(-\omega_0-z) + \mathrm{Res}[\mathcal{G},-\omega_0]\mathcal{G}(-\omega_0+z)\ . \qquad (28)$$

The gap of the two-particle bubbles changed, but it is important that it was increased to $[-\Delta-\omega_0, \Delta+\omega_0]$. The bubbles contain gap states, poles at frequencies $\pm 2\omega_0$. The gap extends to higher values by each convolution of the two-particle propagators. Notice that multiple scatterings in the electron-hole channel contain always a sum of the normal and the anomalous bubble. It follows from the electron-hole symmetry, Eqs. (12) and (13), that the poles from the normal bubble are exactly compensated by the poles in the anomalous bubble. Consequently, the total two-particle bubble $\chi(z)+\psi(z)$ in the electron-hole channel is free of gap singularities.

We now use the normal and anomalous two-particle vertices in the Schwinger-Dyson equations (20) and (21) to determine the normal and anomalous self-energy Σ, $\mathcal{S}$. We single out for this purpose the contribution from the static Hartree-Fock approximation to the self-energy

and introduce a new two-particle function

$$X(i\omega_n, i\nu_m) = \frac{1}{\beta}\sum_{n'} [G(i\omega_{n'})G(i\omega_{n'}+i\nu_m) + \mathcal{G}(i\omega_{n'})\mathcal{G}(i\omega_{n'}+i\nu_m)]\,[K(i\omega_{n'}, i\omega_n; i\nu_m) + \mathcal{K}(i\omega_{n'}, i\omega_n; i\nu_m)] \ . \quad (29)$$

constructed from the normal K and anomalous $\mathcal{K}$ vertices from Bethe-Salpeter equation (19).

From now on we denote $\Sigma(\omega)$ and $\mathcal{S}(\omega)$ the normal and anomalous dynamical self-energies, respectively. That is

$$\begin{aligned} \Sigma(i\omega_n) &= -\frac{U}{\beta}\sum_m G(i\omega_n + i\nu_m)X(i\omega_n, i\nu_m) \ , \\ \Delta_\Phi \mathcal{S}(i\omega_n) &= -\frac{U}{\beta}\sum_m \mathcal{G}(i\omega_n + i\nu_m)X(i\omega_n, i\nu_m) \ . \end{aligned} \quad (30)$$

We find it more convenient to separate the dynamical self-energy from its static part.

We now analytically continue the equations for the self-energy to the spectral representation with real frequencies. Since each convolution increases the gap of the one-electron propagators, we know that the gap of two-particle function X is not smaller than that of the two-particle bubbles. When going over to the spectral representation of the sums over Matsubara frequencies we single out the contribution from the gap states. Using Eq. (24) we obtain a spectral representation for the normal part of the self-energy

$$\Sigma(z) = -U\,\mathrm{Res}[G, -\omega_0]X(z, -\omega_0 - z)f(-\omega_0) - U\,\mathrm{Res}[G, \omega_0]X(z, \omega_0 - z)f(\omega_0) + \Sigma_r(z) \ , \quad (31)$$

where we denoted the contribution to the self-energy from the band states

$$\Sigma_r(z) = U\left[\int_{-\infty}^{-\Delta} + \int_{\Delta}^{\infty}\right]\frac{d\omega}{\pi} f(\omega)\Im G(\omega^+)\omega(z, \omega - z) - U\oint_C \frac{d\zeta}{2\pi i} b(\zeta)G(z+\zeta)X(z,\zeta) \ . \quad (32)$$

Since the analytic structure of function $X(z,\zeta)$ is generally unknown, the contour C of the second integral is defined implicitly so that to involve the bosonic Matsubara frequencies and avoiding singularities of $G(z+\zeta)X(z,\zeta)$ in variable ζ. For the anomalous self-energy we obtain analogously

$$\Delta_\Phi S(z) = -U\,\mathrm{Res}[\mathcal{G}, -\omega_0]X(z, -\omega_0 - z)f(-\omega_0) - U\,\mathrm{Res}[\mathcal{G}, \omega_0]X(z, \omega_0 - z)f(\omega_0) + \Delta_\Phi \mathcal{S}_r(z) \ . \quad (33)$$

with

$$\Delta_\Phi \mathcal{S}_r(z) = U\left[\int_{-\infty}^{-\Delta} + \int_{\Delta}^{\infty}\right]\frac{d\omega}{\pi} f(\omega)\Im \mathcal{G}(\omega^+)X(z, \omega - z) - U\oint_C \frac{d\zeta}{2\pi i} b(\zeta)\mathcal{G}(z+\zeta)X(z,\zeta) \ . \quad (34)$$

We outlined the scheme how individual contributions to the perturbation theory expressed in the Matsubara formalism can be transformed to spectral representations with functions along the axis of real frequencies where we separate the contribution due to the Andreev bound states from those due to the band ones. The convolutions generally split into residues of isolated poles from the energy gap and cuts along the continuum of the band states. Such a decomposition is stable in the perturbation expansion, since the gap edges of the one-particle propagator are independent of the interaction strength and the convolutions can only increase the gap in higher-order functions.

B. Energies of Andreev states

1. Weak-coupling solution

Positions of the Andreev states are explicitly known in the non-interacting case. One expects crossing of these states when the Coulomb repulsion is strong enough. To demonstrate such a behavior one must determine dependence of the energies of the Andreev states on the interaction strength. We know that the energies of the Andreev states are determined by zeros of the determinant of the inverse of the matrix of the full one-electron Green function. Since ABS lie in the gap, the determinant is real and reads for the general spin-symmetric solution

$$D(\omega) = \omega^2\,[1+s(\omega)]^2 - [\epsilon + Un + \Sigma(\omega)]\,[\epsilon + Un + \Sigma(-\omega)] - \Delta_\Phi^2\,[s(\omega) - U\nu - \mathcal{S}(\omega)]\,[s(\omega) - U\nu - \mathcal{S}(-\omega)] \ . \quad (35)$$

The renormalized energy ζ along the real axis $z = \omega \pm i0$ is real outside the energy gap $(-\Delta, \Delta)$ and imaginary within it

$$\begin{aligned} \zeta &= \mathrm{sgn}(\omega)\sqrt{\omega^2 - \Delta^2} \qquad \text{for} \qquad |\omega| > \Delta, \\ \zeta &= \pm i\sqrt{\Delta^2 - \omega^2} \qquad \text{for} \qquad |\omega| < \Delta \ . \end{aligned} \quad (36)$$

The hybridization self-energy is purely imaginary outside the gap and real within it

$$\begin{aligned} s(\omega \pm i0) &= \pm\frac{i\Gamma_0\,\mathrm{sgn}(\omega)}{\sqrt{\omega^2 - \Delta^2}} \qquad \text{for} \qquad |\omega| > \Delta \ , \\ s(\omega \pm i0) &= \frac{\Gamma_0}{\sqrt{\Delta^2 - \omega^2}} \qquad \text{for} \qquad |\omega| < \Delta \ . \end{aligned} \quad (37)$$

Zeros of the determinant $D(\omega)$ define the frequencies of the Andreev states. It is easy to find the defining equation for the energy ω_0 of the Andreev states for the non-interacting dot. From Eq. (16) we directly obtain

$$\omega_0(1 + s_0) = \pm\sqrt{\epsilon^2 + \Delta_\Phi^2 s_0^2} \ . \quad (38)$$

We abbreviated $s_0 = s(\omega_0)$.

2. General spin-symmetric solution

To determine the contributions to the self-energy we need to evaluate the residues of the Green functions in the gap. For the normal and anomalous Green functions the residues at frequency ω are

$$\mathrm{Res}[G,\omega] = \frac{1}{K(\omega)}\left[\omega\left(1+s(\omega)\right)+\epsilon+Un+\Sigma(-\omega)\right], \tag{39a}$$

$$\mathrm{Res}[\mathcal{G},\omega] = -\frac{\Delta_\Phi}{K(\omega)}\left[s(\omega)-U\nu-\mathcal{S}(-\omega)\right] \ . \tag{39b}$$

We denoted the derivative of the determinant $K(\omega) = \partial D(\omega)/\partial\omega$ in the gap. Its explicit representation is

$$\begin{aligned} K(\omega) &= 2\omega\left[1+\frac{\Gamma_0}{\sqrt{\Delta^2-\omega^2}}\right]\left[1+\frac{\Gamma_0\Delta^2}{\left(\Delta^2-\omega^2\right)^{3/2}}\right] \\ &-\big(\Sigma'(\omega)-\Sigma'(-\omega)\big)\big(\epsilon+Un\big)-\big(\Sigma'(\omega)\Sigma(\omega)-\Sigma'(-\omega)\Sigma(-\omega)\big) \\ &-\Delta_\Phi^2\left[\frac{\omega\Gamma_0}{\left(\Delta^2-\omega^2\right)^{3/2}}-\mathcal{S}'(\omega)\right]\Big(s(\omega)-U\nu-\mathcal{S}(-\omega)\Big) \\ &-\Delta_\Phi^2\left[\frac{\omega\Gamma_0}{\left(\Delta^2-\omega^2\right)^{3/2}}+\mathcal{S}'(-\omega)\right]\Big(s(\omega)-U\nu-\mathcal{S}(\omega)\Big) \end{aligned} \tag{40}$$

where prime denotes the frequency derivative. Since $D(-\omega) = D(\omega)$ is an even function of frequency in the spin-symmetric solution, its derivative is an odd function, $K(-\omega) = -K(\omega)$. We assume analyticity of the self-energy at the Fermi level $E_F = 0$. The low-energy asymptotics $\omega \to 0$ of $K(\omega)$ then is $K(\omega) \doteq \omega K_0'$ with

$$\begin{aligned} \frac{K_0'}{2} &= \left[1+\frac{\Gamma_0}{\Delta}\right]^2 - \Sigma''(0)\big(\epsilon+Un\big) - \big(\Sigma'(0)\Sigma(0)\big)' \\ &\quad - \Delta_\Phi^2\left[\frac{\Gamma_0}{\Delta^3}-\mathcal{S}''(0)\right]\left[\frac{\Gamma_0}{\Delta}-U\nu-\mathcal{S}(0)\right] \end{aligned} \tag{41}$$

being a finite number.

Let $\omega_0 \geq 0$ denote the positive frequency of the Andreev state in the spin-symmetric equilibrium state. We resort to zero temperature but do not use any simplifying assumptions there. We denote $s_0^\pm = s(\pm\omega_0)$, $\mathcal{S}_0^\pm = \mathcal{S}(\pm\omega_0)$, $X_0^- = X(-\omega_0,0)$, and $X_{-2}^+ = X(\omega_0,-2\omega_0)$ in the explicit calculations. Moreover, the Green function used in the perturbation expansion is fully renormalized and hence has the same frequencies of the Andreev states as the full Green function, that is $\pm\omega_0$. We single out contributions from the Andreev states to static parameters n and ν and the dynamical self-energy at ω_0. We obtain after analytic continuation

$$n = \frac{\omega_0(1+s_0)-\epsilon-Un-\Sigma_0^+}{K_0} + n_r, \tag{42a}$$

$$\nu = \frac{s_0-U\nu-\mathcal{S}_0^+}{K_0} + \nu_r \ , \tag{42b}$$

$$\Sigma_0^+ = \frac{-\omega_0(1+s_0)+\epsilon+Un+\Sigma_0^+}{K_0}\ UX_{-2}^+ + \Sigma_{0r}^+ \ , \tag{42c}$$

$$\Sigma_0^- = \frac{-\omega_0(1+s_0)+\epsilon+Un+\Sigma_0^+}{K_0}\ UX_0^- + \Sigma_{0r}^- \ , \tag{42d}$$

$$\mathcal{S}_0^+ = \frac{U\nu+\mathcal{S}_0^+-s_0}{K_0}\ UX_{-2}^+ + \mathcal{S}_{r0}^+ \ , \tag{42e}$$

$$\mathcal{S}_0^- = \frac{U\nu+\mathcal{S}_0^+-s_0}{K_0}\ UX_0^- + \mathcal{S}_{r0}^- \tag{42f}$$

where we abbreviated function values $F_0 = F(\omega_0)$. We hid the contributions from the integrals over the band states in unspecified non-singular corrections $n_r, \nu_r, \Sigma_{r0}^\pm$, and $\mathcal{S}_{r0}^\pm$. Notice that generally $\omega_0(1+s_0)-\epsilon-Un-\Sigma_0^+ \geq 0$ as well as $s_0-U\nu-\mathcal{S}_0^+ \geq 0$. The former numerator determines the averaged density of electrons and the latter is proportional to the density of Cooper pairs on the renormalized impurity level ω_0. Both must be nonnegative. It means that the residue cannot cross zero by increasing the interaction strength. They can only reach zero and stay saturated there. That is why the limit $\omega_0 \to 0$ is of importance. The denominator $K_0 \to 0$ and the contributions from the gap states become dominant and we may single them out from the band states.

We decouple and resolve Eqs. (42)

$$n = \frac{\widetilde{\omega}_0-\left[\epsilon+UX_{-2}^+n_r+\Sigma_{r0}^+\right]+K_0n_r}{U+K_0-UX_{-2}^+} \ , \tag{43a}$$

$$\Sigma_0^+ = \frac{UX_{-2}^+\left[-\widetilde{\omega}_0+\epsilon+Un_r\right]+(U+K_0)\Sigma_{r0}^+}{U+K_0-UX_{-2}^+} \ , \tag{43b}$$

$$\Sigma_0^- = \frac{-\widetilde{\omega}_0+\epsilon+Un_r+\Sigma_{r0}^+}{U+K_0-UX_{-2}^+}\ UX_0^- + \Sigma_{r0}^- \ , \tag{43c}$$

$$\nu = \frac{s_0+\left(K_0-UX_{-2}^+\right)\nu_r-\mathcal{S}_{r0}^+}{U+K_0-UX_{-2}^+} \ , \tag{43d}$$

$$\mathcal{S}_0^+ = \frac{UX_{-2}^+\left[U\nu_r-s_0\right]+(U+K_0)\mathcal{S}_{r0}^+}{U+K_0-UX_{-2}^+} \ , \tag{43e}$$

$$\mathcal{S}_0^- = \frac{U\nu_r-s_0+\mathcal{S}_{r0}^+}{U+K_0-X_{-2}^+}\ UX_0^- + \mathcal{S}_{r0}^- \ . \tag{43f}$$

We use the solutions of the equations for n and ν to derive an explicit equation for the frequencies of the

Andreev states. It is easy to find

$$\epsilon + Un + \Sigma_0^+ = \frac{U(1-X_{-2}^+)\widetilde{\omega}_0 + \left[\epsilon + Un_r + \Sigma_{r0}^+\right] K_0}{U + K_0 - UX_{-2}^+} \ , \quad (44a)$$

$$\epsilon + Un + \Sigma_0^- = \epsilon + Un + s_0^+ + \Sigma_{r0}^- - \Sigma_{r0}^+ + U\frac{-\widetilde{\omega}_0 + \epsilon + Un_r + \Sigma_{r0}^+}{U + K_0 - UX_{-2}^+}\left(X_0^- - X_{-2}^+\right) \ , \quad (44b)$$

$$s_0 - U\nu - \mathcal{S}_0^+ = \frac{s_0 - U\nu_r - \mathcal{S}_{r0}^+}{U + K_0 - UX_{-2}^+} \ K_0 \ , \quad (44c)$$

$$s_0 - U\nu - \mathcal{S}_0^- = \mathcal{S}_{r0}^+ - \mathcal{S}_{r0}^- + \frac{s_0 - U\nu_r - \mathcal{S}_{r0}^+}{U + K_0 - UX_{-2}^+}\left(K_0 + UX_0^- - UX_{-2}^+\right) \ . \quad (44d)$$

We can now write an equation for the zeros of determinant $D(x)$ from Eq. (35), $x = \omega_0$. In the limit $\omega_0 \to 0$ we have $\Sigma_{r0}^+ - \Sigma_{r0}^- = 2\omega_0\Sigma_r(0)'$, $\mathcal{S}_{r0}^+ - \mathcal{S}_{r0}^+ = 2\omega_0\mathcal{S}_r(0)'$, and $X_0^- - X_{-2}^+ = 2\omega_0\left(\partial_R - \partial_L\right)X(\omega_L,\omega_R)|_{\omega_{L,R}=0}$, where $\partial_{L,R}$ indicates the partial derivative in the left (ω_L), right (ω_R) variable, respectively. The only assumption made is analyticity of the self-energy $\Sigma(\omega)$ and of the reduced vertex $X(\omega_L,\omega_R)$ at the Fermi energy $E_F = 0$. Determinant $D(\omega_0)$ is then proportional to ω_0^2 in the limit$\omega_0 \to 0$

$$D(\omega_0) = \omega_0^2\left\{\left(1+\frac{\Gamma_0}{\Delta}\right)^2 - \left[1+\frac{\Gamma_0}{\Delta} + \frac{\epsilon + Un_r + \Sigma_r^0}{U(1-X_{00})}\ K_0'\right]\left[1+\frac{\Gamma_0}{\Delta} + \frac{\epsilon + Un_r + \Sigma_r^0}{U(1-X_{00})}\left(K_0' + 2U\partial_R X_{00} - 2U\partial_L X_{00}\right)\right.\right.$$
$$\left.\left. - 2\Sigma_r^{0\prime}\right] - \Delta_\Phi^2 K_0' \ \frac{\Gamma_0/\Delta - U\nu_r - \mathcal{S}_r^0}{U(1-X_{00})}\left[\frac{\Gamma_0/\Delta - U\nu_r - \mathcal{S}_r^0}{U(1-X_{00})}\left(K_0' + 2U\partial_R X_{00} - 2U\partial_L X_{00}\right) + 2\mathcal{S}_r^{0\prime}\right]\right\} + O(\omega_0^4) \ . \quad (45)$$

We denoted the values of the one-electron functions at the Fermi energy with an upper index 0. Further on, $X_{00} = X(0,0)$. We see that $\omega_0 = 0$ is a solution for the frequencies of the Andreev states. The expression within the braces is generally nonzero. The solution $\omega_0 = 0$ exists, however, only if consistency conditions are obeyed, that is $0 \le n \le 1$. They explicitly read

$$0 \le -\left[\epsilon + UX_{00}n_r + \Sigma_r^0\right] \le U - X_{00} \ . \quad (46)$$

The two static parameters in the solution with $\omega_0 = 0$ are

$$n = -\frac{\epsilon + UX_{00}n_r + \Sigma_r^0}{U(1-X_{00})} \ , \quad (47a)$$

$$\nu = \frac{\Gamma_0/\Delta - UX_{00}\nu_r - \mathcal{S}_r^0}{U(1-X_{00})} \ . \quad (47b)$$

The self-energy for the solution with $\omega_0 = 0$ is

$$\Sigma(z) = -\frac{UX(z,-z)}{2\left[1+\Gamma/\Delta + \Sigma_0'\right]} + \Sigma_r(z), \quad (47c)$$

$$\mathcal{S}(z) = \mathcal{S}_r(z) \ , \quad (47d)$$

since the anomalous Green function does not have poles in the gap. We used Eq. (41) to determine the residue of the (double) pole in the normal Green function. Equation (47c) induces an equation for Σ_0'

$$2\left(\Sigma_0' - \Sigma_{r0}'\right) = \frac{U\left(\partial_R - \partial_L\right)X_{00}}{1+\Gamma/\Delta + \Sigma_0'} \ . \quad (47e)$$

All equations (47) for static parameters n, ν, Σ_0' and functions $\Sigma(\omega)$ and $\mathcal{S}(\omega)$ must be solved simultaneously to determine the solution with the Andreev states pinned at the Fermi energy. Such a solution is bounded in the Coulomb repulsion from below, since inequalities in Eq. (46) must be obeyed. It may also be bounded from above by a singularity in vertex X. Such singularity would indicate a continuous transition to a spin-polarized solution. The solution with $\omega_0 = 0$ is an isolated point that is very sensitive to magnetic fluctuations. Its stability can be investigated only if external magnetic field is applied and the spin symmetry broken. It is, however, beyond the scope of this paper.

Notice that the limits $\omega_0 \to 0$ and $T \to 0$ do not commute. Equations (47) hold for the order $\omega_0 \to 0$ followed by $T \to 0$. The solution with $\omega_0 = 0$ exists independently of the solution with $\omega_0 > 0$ if inequalities in Eq. (46) are obeyed. The latter solution exists in the weak-coupling regime where the expression within the braces of Eq. (45) is non-zero (negative). With increasing interaction the leading term of the expansion in ω^2 of determinant $D(\omega)$ approaches zero. At a critical interaction it vanishes and the Andreev states reach the Fermi energy. Beyond this interaction there is no solution for (real) nonzero frequencies of the Andreev states. The gap states remain frozen at the Fermi energy. The critical interaction strength at which the Andreev states reach the Fermi energy is determined form the following

equation

$$U(1-X_{00})\left\{-2\left(1+\frac{\Gamma_0}{\Delta}\right)\left[\epsilon+Un_r+\Sigma_r^0\right](K_0'+U\partial_R X_{00}-U\partial_L X_{00})\,U(1-X_{00})+2\Sigma_r^{0\prime}\left[\left(1+\frac{\Gamma_0}{\Delta}\right)U(1-X_{00})\right.\right.$$
$$\left.\left.+(\epsilon+Un_r+\Sigma_r^0)K_0'\right]\right\}-(\epsilon+Un_r+\Sigma_r^0)^2K_0'(K_0'+2U\partial_R X_{00}-2U\partial_L X_{00})-\Delta_\Phi^2K_0'\left(\frac{\Gamma_0}{\Delta}-U\nu_r-\mathcal{S}_r^0\right)$$
$$\times\left[\left(\frac{\Gamma_0}{\Delta}-U\nu_r-\mathcal{S}_r^0\right)(K_0'+2U\partial_R X_{00}-2U\partial_L X_{00})+2\mathcal{S}_r^{0\prime}\right]=0\ . \quad (48)$$

The solution with $\omega_0>0$ develops from the solution of the noninteracting dot and determines the 0-phase. Frequency ω_0 is the energy we win when a Cooper pair is created on the dot. This solution at zero temperature saturates at a critical interaction U_c at which the density of Cooper pairs reaches extremum, $s_0-U\nu-\mathcal{S}_0=0$ and creation and annihilation of Cooper pairs costs no energy. Saturation indicates degeneracy of the ground state and emergence of a new state. A quantitative description of this new phase beyond the critical point demands, however, introduction of a perturbation theory for a degenerate ground state. This is beyond the scope of this approach in which we assumed a spin-symmetric and non-degenerate many-body ground state.

The two solutions, $\omega_0>0$ and $\omega_0=0$, may coexist. The solution with $\omega_0>0$ exists in the weak-coupling region $U<U_c$, where the critical interaction U_c is determined in Eq. (48). The solution with $\omega_0=0$ exists in the strong-coupling region $U>U_0$ where the boundary interaction U_0 is determined from the right equality in Eq. (46). Both solutions in the coexistence region $U_0<U<U_c$ are saddle points of the free energy functional. One of them is the true ground state. The transition between the two solutions at zero temperature is continuous if the weak-coupling state with $\omega_0>0$ remains stable up to the critical interaction U_c. One needs to know the free-energy functional to decide this question and to determine the transition point at non-zero temperatures were the critical interaction $U_c(T>0)=\infty$.

V. ANDREEV STATES IN THE WEAK-COUPLING REGIME

We demonstrate explicitly the universal existence of the critical interaction from the general theory on dynamical approximations in the weak-coupling regime. We use approximations with a self-energy calculated from second-order perturbation theory or from multiple electron-hole scatterings (RPA). The former is a simplification of the latter. To determine dynamical corrections to the static Hartree-Fock approximation we must evaluate the reduced two-particle vertex $X(i\omega_n,i\nu_m)$ defined in Eq. (29). The full two-particle vertices $K(i\omega_n,i\omega_{n'};i\nu_m)$ and $\mathcal{K}(i\omega_n,i\omega_{n'};i\nu_m)$ are determined from a Bethe-Salpeter equation diagrammatically represented in Eq. (19). The simplest approximation, the electron-hole ladder, uses the bare interaction as the the irreducible vertex, $L=U$. The anomalous irreducible vertex then is zero, $\mathcal{L}=0$. The matrix Bethe-Salpeter equation reduces to a couple of algebraic equations for the normal and anomalous vertices K and $\mathcal{K}$. They are

$$K(i\nu_m)=U-U\chi(i\nu_m)K(i\nu_m)-U\psi(i\nu_m)\mathcal{K}(i\nu_m) \quad (49a)$$

and

$$\mathcal{K}(i\nu_m)=-U\psi(i\nu_m)K(i\nu_m)-U\chi(i\nu_m)\mathcal{K}(i\nu_m)\ . \quad (49b)$$

The two equations can be decoupled and we obtain explicit solutions

$$K(i\nu_m)=\frac{U}{1+U\chi(i\nu_m)-\dfrac{U^2\psi(i\nu_m)^2}{1+U\chi(i\nu_m)}}\ , \quad (50a)$$

$$\mathcal{K}(i\nu_m)=-\frac{U\psi(i\nu_m)}{1+U\chi(i\nu_m)}\,K(i\nu_m)\ . \quad (50b)$$

The vertex needed for the dynamical self-energy then is

$$X(i\omega_n,i\nu_m)=U[\chi(i\nu_m)+\psi(i\nu_m)]\times\frac{1+U\chi(i\nu_m)-U\psi(i\nu_m)}{[1+U\chi(i\nu_m)]^2-U^2\psi(i\nu_m)^2}$$
$$=U\,\frac{\chi(i\nu_m)+\psi(i\nu_m)}{1+U\left[\chi(i\nu_m)+\psi(i\nu_m)\right]}\ . \quad (51)$$

We now use this vertex function to determine the normal and anomalous self-energy, Eqs. (31) and (33), that at zero temperature read

$$\Sigma(z)=-UX(z,-\omega_0-z)\,\mathrm{Res}[G,-\omega_0]+\Sigma_r(z)\ , \quad (52a)$$

$$\Delta_\Phi\mathcal{S}(z)=-UX(z,-\omega_0-z)\,\mathrm{Res}[\mathcal{G},-\omega_0]+\Delta_\Phi\mathcal{S}_r(z)\ . \quad (52b)$$

They determine together with the equations for the static parameters n and ν our approximation for $\omega_0 > 0$. The other solution with $\omega_0 = 0$ is determined from Eqs. (47).

We resolved numerically Eq. (51) and Eq. (52) in the weak-coupling regime for interaction strengths with no pole in the two-particle vertex $K(\omega)$. To expedite convergence we used a simplified self-consistency in the above equations. The one-electron propagators in Eq. (51) use a static self-energy of the Hartree-Fock type in a dynamical environment so that the frequencies of the Andreev states are the same as those of the resulting full propagator. The effective dynamical environment is defined by the first iteration of the full dynamical self-consistency. This simplification does not deteriorate the full approximation significantly as demonstrated in Ref. 30. What is of principal importance is the self-consistency in the frequencies of the Andreev states. Otherwise the saturation at the Fermi energy is not reached.

We calculated the behavior of the Andreev states in three weak-coupling approximations, static Hartre-Fock and dynamical second-order and the ladder of multiple electron-hole scatterings. We also applied Numerical Renormalization Group technique to determine the reference for the behavior of the Andreev states at zero temperature.[35,36] We plotted the frequencies of the Andreev states as a function of the Coulomb repulsion at the charge-symmetric situation in Fig. 2. We see that all three approximations display the same qualitative behavior derived generally in the preceding section. Only the critical interaction differs in these approximations. We already know that second order approximation gives a very accurate values for the frequencies of the Andreev states,[30] hence one does not expect significant deviations from them. The difference between the RPA and second order will be then compensated by multiple scatterings of electron pairs. We used only moderate interaction strengths for the zero phase, below the RPA unphysical pole ($U_c \approx 3 \sim 4\Delta$ depending on ε and Φ) indicating a transition to a magnetic state.

The behavior of the Andreev states as a function of the impurity energy level is plotted in Fig. 3. Here we can see the region where there is no solution with nonzero frequency and only Andreev states with $\omega_0 = 0$ exist. The Hartree-Fock solution does not yet show the saturation at the chosen value of the interaction strength $U = 3\Delta$. The corresponding electron density is plotted in Fig. 4 where we indicated the coexistence region for the solutions with $\omega_0 > 0$ and $\omega_0 = 0$. The latter solution spans the whole spectrum of electron densities between $n = 0$ (right edge) and $n = 1$ (left edge). Only the solution of the ladder approximation is plotted. The dependence of the frequencies of the Andreev states as a function of the phase difference between the superconducting leads is plotted in Fig. 5. The behavior is very similar to that from Fig. 2. Increasing the phase difference enhances the effect of the Coulomb repulsion.

Our numerical calculations confirmed the general conclusion about the behavior of the spin-symmetric solution. The frequencies of the Andreev states approach the Fermi energy with increasing interaction strength. They merge at the Fermi energy at a critical interaction U_c above which only the solution with the Andreev states pinned at the Fermi energy exists. It is important to guarantee in approximate calculations that the frequency of the Andreev states of the Green function used in the equation for the full self-energy, Eq. (52), are identical with the energies calculated with the Green function and the self-energy from Eq. (52). If this condition is not fulfilled, fluctuations in the values of the frequencies of the Andreev states in iterations prevent reaching a stable equilibrium state.

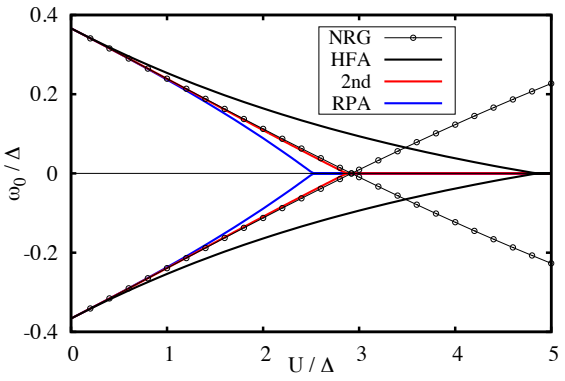

FIG. 2: (Color online) Frequencies of the Andreev states in the spin-symmetric solution as a function of Coulomb repulsion. Different weak-coupling approximations were compared to demonstrate universality of saturation of the spin-symmetric solution and the NRG data were used as a reference for determining the actual crossing of Andreev states. Input parameters are $\Gamma = \Delta$, $\epsilon = -U/2$ and $\Phi = \pi/2$.

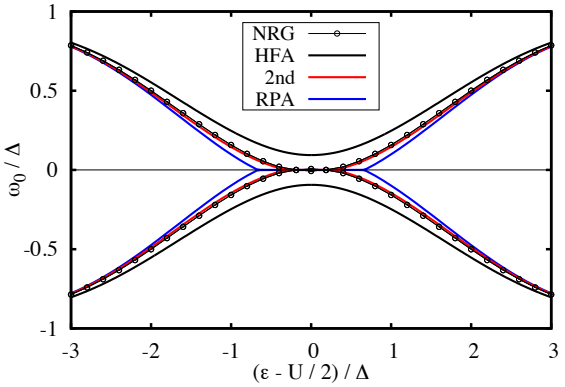

FIG. 3: (Color online) Frequencies of the Andreev states in the spin-symmetric solution as a function of atomic energy level ϵ. Input parameters are $\Gamma = \Delta$, $U = 3\Delta$ and $\Phi = \pi/2$. The NRG data in the π-phase are too close to zero to discern the crossing.

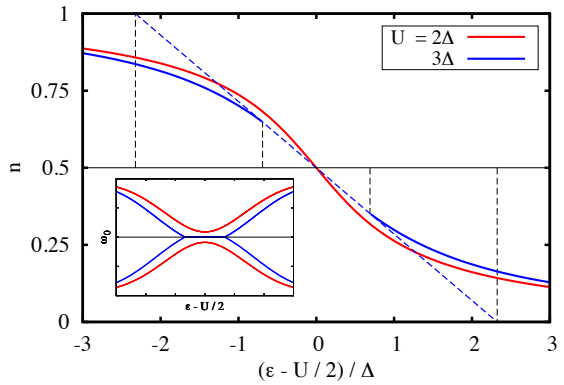

FIG. 4: (Color online) Electron density as a function of atomic energy level ϵ for two values of the interaction strength. Limits on solution with $\omega_0 > 0$ (solid line) and $\omega_0 = 0$ (dashed line) are indicated. Input parameters are $\Gamma = \Delta$ and $\Phi = \pi/2$. The inset shows the frequencies of the corresponding Andreev states.

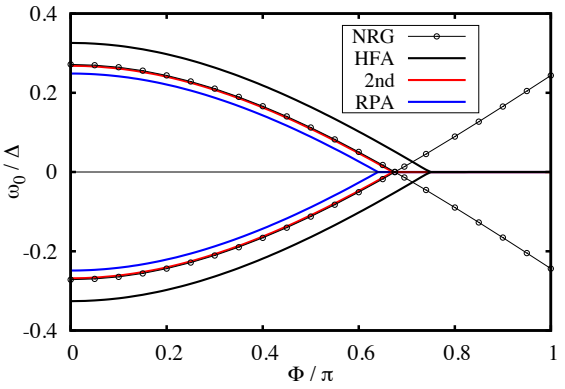

FIG. 5: (Color online) Frequencies of the Andreev states in the spin-symmetric solution as a function of phase difference Φ. Input parameters are $\Gamma = \Delta$, $U = 2\Delta$ and $\epsilon = -\Delta$.

VI. CONCLUSIONS

We studied in this paper the many-body perturbation theory of a single impurity attached to two superconducting leads. The perturbation expansion was done in the on-site Coulomb repulsion assuming non-degenerate spin-symmetric equilibrium (ground) state. Although formulated in the Matsubara formalism, the expansion terms were analytically transformed to real frequencies so that to be able to control the behavior of the Andreev states. The general trend in the dependence of the Andreev bound states on the Coulomb repulsion is known, they approach the Fermi energy. Numerical studies then predict a crossing of the Andreev states at the Fermi energy signaling the $0-\pi$ transition. This transition should not be accompanied by breaking of the spin-reflection symmetry, that is by a transition to a magnetic state. A simple static mean-field approach leads to a discontinuous $0-\pi$ transition induced by a magnetic order on the impurity. The aim of our study was to determine the impact of dynamical corrections and to find whether the spin-symmetric solution allows for crossing of Andreev states and is able to describe both 0 and π phase reliably.

A recent study[30] demonstrated importance of dynamical corrections. It showed that in the weak-coupling regime the Andreev states at zero temperature reach the Fermi energy and this point was identified as the boundary of the 0-phase beyond which only the π-phase may exist. The approach from Ref. 30 cannot be extended into the π-phase and hence gives no clue to the behavior of the Andreev states there. We extended this weak-coupling analysis of the spin-symmetric solution to arbitrary interaction strengths. We analyzed the behavior of the Andreev states in the vicinity of the Fermi energy generally. We were able to find the exact asymptotic behavior of the one-electron impurity Green function in the limit of vanishing frequency of the Andreev states. We found that Andreev states at zero-temperature always reach the Fermi energy at a critical interaction strength U_c in the spin-symmetric solution. Above this critical interaction there is only a solution with Andreev states pinned at the Fermi energy. We hence concluded that a continuous crossing of Andreev states in the spin-symmetric solution is not possible.

The solution with Andreev states pinned at the Fermi energy can exist independently from the one with separated Andreev states. The existence of the former solution is bounded from below. It can exist only above a certain interaction strength $U_0 < U_c$ and hence the two solutions coexist on this interval. The solution with Andreev states pinned at the Fermi energy is not perturbative and forms an isolated state within the spin-symmetric phase space. It is sensitive to the external magnetic field that lifts its degeneracy. It is stable only if the linear response to the external magnetic field, breaking the spin symmetry, holds. In the simplest Hatree-Fock approximation the merging of Andreev states at the Fermi energy is preceded by a discontinuous transition to a magnetic state. Stability of solutions with dynamic fluctuations with respect to magnetic fluctuations remains to be investigated. The genesis of the the true π-phase and the behavior of the Andreev states at the transition can hence be answered only if an external magnetic field is applied and and stability of various solutions with respect to its variations is studied.

Acknowledgment

We thank T. Novotný for valuable discussions on the physics of the quantum dot attached to two superconducting leads. Research on this problem was supported in part by Grant P204-11-J042 of the Czech Science Foundation. VJ thanks The Fulbright Visiting Scholar Pro-

gram for financing his stay at Louisiana State University.

---

* Electronic address: janis@fzu.cz

[1] S. De Franceschi, L. Kouwenhoven, C. Schönenberger, and W. Wernsdorfer, Nature Nanotech. **5**, 703 (2010).

[2] A. Martín-Rodero and A. Levy Yeyati, Adv. Phys. **60** 899 (2011).

[3] P. Jarillo-Herrero, J. A. van Dam, and L. P. Kouwenhoven, Nature **439**, 953–956 (2006).

[4] H. I. Jørgensen, K. Grove-Rasmussen, T. Novotný, K. Flensberg, and P. E. Lindelof, Phys. Rev. Lett. **96**, 207003 (2006).

[5] H. I. Jørgensen, K. Grove-Rasmussen, K. Flensberg, and P. E. Lindelof, Phys. Rev. B **79**, 155441 (2009).

[6] J. A. van Dam, Y. V. Nazarov, E. P. A. M. Bakkers, S. De Franceschi and L. P. Kouwenhoven, Nature **442**, 667 (2006).

[7] J. P. Cleuziou, W. Wernsdorfer, V. Bouchiat, T. Ondarcuhu, and M. Monthioux, Nature Nanotech. **1**, 53 (2006).

[8] H. I. Jørgensen, T. Novotný, K. Grove-Rasmussen, K. Flensberg, P. E. Lindelof, Nano Lett. **7**, 2441–2445 (2007).

[9] A. Eichler *et al.* Phys. Rev. B **79**, 161407 (2009).

[10] R. Maurand *et al.* Phys. Rev. X **2**, 011009 (2012).

[11] L. I. Glazman and M. E. Raikh, JETP Lett. **47**, 452 (1988).

[12] A. V. Rozhkov and D. P. Arovas, Phys. Rev. Lett. **82**, 2788 (1999).

[13] E. Vecino, A. Martín-Rodero and A. Levy Yeyati, Phys. Rev. B **68**, 035105 (2003).

[14] Martín-Rodero, A. & Yeyati, A. L. J. Phys.: Condens. Matter **24**, 385303 (2012).

[15] M.-S. Choi, M. Lee, K. Kang, and W. Belzig, Phys. Rev. B **70**, 020502(R) (2004).

[16] A. Oguri, Y. Tanaka, and A. C. Hewson, J. Phys. Soc. Jpn. **73**, 2494 (2004).

[17] J.-D. Pillet, P. Joyez, R. Žitko, M. F. Goffman, Phys. Rev. B **88**, 045101 (2013).

[18] F. Siano and R. Egger, Phys. Rev. Lett. **93**, 047002 (2004).

[19] D. J. Luitz and F. F. Assaad, *Physical Review B* **81**, 024509 (2010).

[20] L. I. Glazman and K. A. Matveev, JETP Lett. **49**, 659 (1989).

[21] T. Novotný, A. Rossini, and K. Flensberg, Phys. Rev. B **72**, 224502 (2005).

[22] T. Meng, S. Florens, and P. Simon, Phys. Rev. B **79**, 224521 (2009).

[23] A. A. Clerk and V. Ambegaokar, Phys. Rev. B **61**, 9109–9112 (2000).

[24] G. Sellier, T. Kopp, J. Kroha, and Y. S. Barash, Phys. Rev. B **72**, 174502 (2005).

[25] C. Karrasch, A. Oguri and V. Meden, Phys. Rev. B **77**, 024517 (2008).

[26] J. Bauer, A. Oguri, and A. C. Hewson, J. Phys.: Condens. Matter **19**, 486211 (2007).

[27] T. Hecht, A. Weichselbaum, J. von Delft, and R. Bulla, J. Phys.: Condens. Matter **20**, 275213 (2008).

[28] J. S. Lim and M. S. Choi, J. Phys.: Condens. Matter **20**, 415225 (2008).

[29] J.-D. Pillet, C. Quay, P. Morfin, C. Bena, A. Levy Yeyati, P. Joyez, Nature Phys. **6** 965 (2010).

[30] M. Žonda, V. Pokorný, V. Janiš, and T. Novotný, Scientific Reports **5**, 8821 (2015).

[31] D. J. Luitz, F. F. Assaad, T. Novotný, C. Karrasch, and V. Meden, Phys. Rev. Lett. **108**, 227001 (2012).

[32] V. Janiš, in *Open Problems in Strongly Correlated Electron Systems*, NATO Science Series II. Mathematics, Physics and Chemistry - vol. 15, J. Bonča, P. Prelovšek, A. Ramšak, and S. Sarkar eds. (Kluwer Academic Publishers, Dordrecht, 2000).

[33] V. Janiš, Phys. Rev. B **60**, 11345 (1999).

[34] V. Janiš and V. Pokorný, ScienceJet **3**, 66 (2014).

[35] R. Žitko, NRG Ljubljana - open source numerical renormalization group code (2014). http://nrgljubljana.ijs.si.

[36] R. Žitko and T. Pruschke, Phys. Rev. B **79**, 085106 (2009).